Supplementary material

Material and methods

Isolation of endothelial cells from brain tissue

Tissue was mechanically dissociated using scissors, followed by enzymatical dissociation in HBSS (Gibco, 14065-049) containing 1.55 g/L glucose, 0.08 WU/mL Liberase DH (Sigma, 5401054001) and 100 U/mL DNaseI (Sigma, D4263-5VL) at 37 °C for 60 minutes (1 ml per 100 mg of tissue). After the dissociation, the lysed tissue was passed through a 100 µm mesh and washed with HBSS containing 1% BSA, 1.55 g/L glucose and 100 U/ml DNaseI. Tissue lysate was mechanically dissociated by pipetting 40 times using a 1000mL pipette with subsequent passage through a 40 µm mesh, and then centrifuged for 5 minutes at 300g at 4 °C. The cell pellet was resuspended in the isolation buffer containing PBS w/o $Ca2^{+}$ and $Mg2^{+}$, 0.1% BSA and 2mM EDTA pH 7.4. To enrich the samples for endothelial cells, we initially performed a negative selection by adding 25 µl/ml of anti-CD15 antibody (Ab) (Invitrogen, 11137D), and anti-CD45 Ab (Invitrogen, 11153D) conjugated Dynabeads and incubated at 12 °C on a shaking device (Eppendorf ThermoMixer C) for 30 minutes. CD45 and CD15 positive cells were removed using a magnetic particle concentrator rack (DynaMag™-5 Magnet; Invitrogen; 12303D). The tissue lysate was centrifuged at 300g, for 10 minutes at 4 °C. The cell pellet was resuspended in isolation buffer 2 (HBSS, 1% BSA, 1.55 g/L glucose) and incubated with 25 µl/ml anti-CD31 Dynabeads (Invitrogen, 11155D) solution for 20 minutes at 12 °C and constant movement (300rpm, Eppendorf ThermoMixer C). CD31 positive endothelial cells were isolated using an MPC rack, which was repeated twice to capture all anti-CD31-Ab labelled cells. Cells were washed with isolation buffer 2 and PBS, then lysed for RNA isolation.

Immunohistochemistry

GBM and control samples were embedded in OCT freezing medium (CellPath, 81-0771-00) and 10 µm thick slices were cut with a Leica CM 1850 UV Cryostat. Slices were cut at -25 °C and picked up with TOMO glass slides (Matsunami, TOM-1190, 75x25x1mm). After drying, the slides were stored at -20 °C until used for immunohistochemistry. For on-slide stainings, all steps were performed in a humidity chamber. Tissue slices were incubated in blocking solution (Superblock, ThermoFisher, 37535) for 30 minutes at room temperature (RT), followed by overnight incubation of primary antibodies

(Supplementary Table 1) at 4 °C. Samples were washed with PBS, 0.01% Tween 20 and incubated with fluorescently-labelled secondary antibodies for 2h at RT. All secondary antibodies (anti-rabbit, anti-mouse, and anti-goat) made in donkey conjugated to fluorophores (Alexa 488, Cy3, DyLight 649) suitable for multiple labelling were purchased from Jackson Immunoresearch. Cell nuclei were visualized using the 4′,6-Diamidin-2-phenylindol (DAPI). Samples were mounted in Prolong Gold Antifade Mounting Reagent (Invitrogen, cat # P36930). Imaging was preformed using a SP5 laser scanning confocal microscope equipped with a 20x objective (numerical aperture 0.7) (Leica). For image processing, Imaris (Bitplane) software was used. For imaging and image processing, the same settings were used for GBM and control samples.

Quantification of immunohistochemistry images

Quantification of fluorescence images was performed using FIJI (ImageJ) software. Channels were opened separately and Z-Projection (Sum Slices) was performed. For CD31 staining, a binary image was prepared and if necessary, a median filter was applied to reduce salt and pepper noise. The CD31 binary image was used to create a selection, which was then transferred to the second channel using the ROI (Region of Interest) manager. Mean grey value was calculated from this ROI (i.e. CD31 positive area). To quantify perivascular fibroblasts, the polygon tool was used to create a ROI around the CD31 positive area. These ROIs were transferred to the channel of ADAM12 and CLEC3B and mean grey value was measured in the ROI.

Bioinformatics analysis of RNA seq data

Raw reads in fastq sequencing files were cleaned to remove Illumina adapters and low quality reads with Trimmomatic (v.0.36) [1]. Trimmed reads were then aligned against the human reference genome (GRCh38.p10, annotation release 89, 2017-05-31) using the STAR aligner (v.2.5.3a) [2]. Alignment files were sorted using Samtools (v.1.5) [3]. Reads per gene locus were counted using featureCounts in the Rsubread package [4] for R (v.3.4.2). Number of reads and gene biotypes of each sample are listed in Supplementary Table 2. Normalization and differential gene expression analysis was performed on the counts data using R (v.3.5.3) and the DESeq function of the DESeq2 package [5] for R, with default parameters. We tested for differential gene expression between GBM and control samples, and between lung adenocarcinoma metastasis and control samples separately. Genes were considered as

significantly differentially expressed at adjusted p-value <0.05. Gene set overrepresentation analysis of Gene Ontology biological process [6,7] gene sets was performed using the enrichGO implemented in the clusterProfiler package [8]. This overrepresentation analysis was used for DEG identified in GBM *versus* control or BM *versus* control, but also for genes that were in common or not between GBM and BM.

To determine cell-type specific enrichment in either GBM or BM, we used smaller cell-type specific gene sets, applying gene set enrichment analysis (GSEA; [9]. Briefly, all genes were sorted according to their Wald statistic, and up- or downregulated genes were tested separately. For each gene set, an enrichment score (ES) was calculated by increasing or decreasing a running-sum statistic proportionally to the magnitude of the Wald statistic of each gene (using p=1, see Equation 1 in Subramanian et al.). Randomized ES values were calculated by randomizing gene labels 1000 times. The normalized enrichment score (NES) was calculated by dividing the ES by the mean of the 1000 randomized ES values. A p-value associated to each NES was determined based on the proportion of randomized ES values that had a higher (for positive ES) or lower (for negative ES) value than the ES initially calculated. P-values were finally adjusted using the Benjamini-Hochberg procedure [10] GSEA was performed using two gene sets. One consisted of mouse-derived marker genes of fibroblasts, mural cells, astrocytes, oligodendrocytes, microglia and endothelial cells. Another gene set consisted of key pathways involved in the maturation of the mouse BBB (gene sets of Figure 5 and Figure 6 in [11]).

Analysis of DEG in GBM EC in the IVY GAP

Normalized gene-level FPKM (Fragments Per Kilobase of transcript per Million mapped reads) values were downloaded from the IVY GAP [12], webpage (https://glioblastoma.alleninstitute.org/static/download.html; zipped folder “gene_expression_matrix_2014-11-25”). Only samples originating from reference histology GBM regions were retained (cellular tumor (CT), microvascular proliferation (CTmvp), pseudopalisading cells around necrosis (CTpan), infiltrating tumor (IT) and leading edge (LE)). Within a heatmap created with the ComplexHeatmap package (v. 1.20.0) for R [13], only genes differentially expressed between our GBM and control samples were hierarchically clustered according to their expression pattern in IVY GAP tumor regions (complete hierarchical clustering method using Euclidean distance). Subsets of genes with high average z-score values in LE+IT or in MVP but low values in other regions were selected and subjected to gene set overrepresentation analysis against the Gene Ontology biological process gene sets, using the enrichGO function of the clusterProfiler package (v. 3.10.1) [8].

Determination of CD31-positive endothelial cell sample enrichment using Genotype-Tissue Expression (GTEx) data

To determine whether we had successfully enriched our samples with CD31-positive endothelial cells or not, we compared our samples to bulk brain samples available in the GTEx project (https://gtexportal.org/home/). Because the number of samples per tissue is higher in the GTEx project than in our RNA seq data, we randomly selected 6 samples in each of 3 bulk brain tissues available in the GTEx project: Hippocampus, cortex and the putamen of the basal ganglia (gene read counts and sample attributes downloaded from GTEx v7 on 02/25/2019). The sample IDs of the GTEx cortex samples were: GTEX-Z93S-2926-SM-57WB9, GTEX-13O3O-3126-SM-5KM3H, GTEX-Y111-2726-SM-4TT3N, GTEX-1445S-3026-SM-5O9BR, GTEX-11GS4-3126-SM-5A5LH and GTEX-144FL-3026-SM-5O99C. The sample IDs of the GTEx hippocampus samples were: GTEX-13JVG-0011-R1a-SM-5KM32, GTEX-PVOW-0011-R1A-SM-32PL6, GTEX-13N1W-0011-R1b-SM-5MR4T, GTEX-13FLW-0011-R1b-SM-5LZX2, GTEX-OHPN-0011-R1A-SM-2I5GB and GTEX-139TT-0011-R1a-SM-5LZVD. The sample IDs of the GTEx putamen of the basal ganglia samples were: GTEX-14PJO-0011-R7a-SM-664NR, GTEX-13O3O-0011-R7b-SM-5P9GZ, GTEX-RNOR-0011-R7A-SM-2TF4V, GTEX-ZAB4-0011-R7a-SM-4SOKE, GTEX-NL3H-0011-R7a-SM-2I3G5 and GTEX-N7MS-0011-R7a-SM-2HMKN. GTEx gene counts were merged with our RNA seq raw counts and filtered to only retain genes with at least 1 count per million (cpm) in 1 sample. Gene counts were normalized using the trimmed mean of M values (TMM) method implemented in the edgeR (v. 3.24.3) package for R [14], and converted to $\log_2$ cpm using the voom function of the limma (v. 3.38.3) package [15]. Next, differential gene expression analysis was performed among and between each GTEx brain tissue type and our control and tumor RNA seq tissues by fitting a linear model using limma. Finally, a list of EC marker genes was extracted from Figure 2A of Butler et al. [16], GSEA [9] was used to calculate an enrichment score for this EC marker gene list among or between each GTEx brain tissue type and our control and tumor RNA seq tissues. If our CD31-positive endothelial cell enrichment was successful, we expected a high enrichment score for our tumor and control RNA seq samples when compared to the GTEx samples, but a negligible enrichment score among GTEx samples or among RNA seq samples.

Comparison to previously published gene expression data

By extracting gene lists associated with GBM in the literature, we calculated an enrichment score for each of our GBM, metastasis or control samples separately. This allowed us to determine how well each sample's gene expression was matching the pattern of published deregulated genes in GBM. The enrichment score [17] was the sum of the z-scores of the upregulated genes minus the sum of the z-scores of the downregulated genes (if present).

One gene list for which we calculated this enrichment score was defined as a core BBB dysfunction module in mouse (Figure 5a in Munji et al.) [18]. A second gene list was defined using microarray data of micro-dissected vessels of gliomas and healthy control, including both upregulated and downregulated genes in gliomas (Supplementary Table 2 of Dieterich et al.) [19]. Finally, we calculated an enrichment score using GBM EC- or normal EC-associated genes determined by correlation analyses in Dusart et al. (Supplementary Table 8, tab 3) [20]. GBM EC-associated genes were the ones having a mean correlation coefficient >0.5 in GBM and <0.5 in normal EC, and normal EC-associated genes were the ones having a mean correlation coefficient <0.5 in GBM and >0.5 in normal EC.

Supplementary results and discussion

DEG in GBM endothelial cells are enriched in specific tumor anatomical structures

EC were isolated from GBM resection material, which lacked positional information about anatomical tumor regions. Thus, our dataset includes EC originating from all tumor regions. Because different tumor regions show distinct gene expression profiles, we determined whether the DEG we identified in our study were specific to some particular GBM regions. Using the Ivy Glioblastoma Atlas Project (IVY GAP) RNAseq data obtained from anatomically different GBM regions [12], we found that our list of DEG included genes that were highly expressed in several anatomical regions of GBM (Supplementary Fig. 5-7). We focused on a subset of DEG that were more expressed in the IVY GAP dataset in the leading edge (LE) and infiltrating tumor (IT) region, and microvessel-proliferation (MVP) region. GO-overrepresentation analysis of genes downregulated in GBM EC but preferentially expressed in LE and IT region (105 genes) in GBM tissue identified gene sets that are associated with blood circulation, circulatory system and import across plasma membrane (Supplementary Figure 5A, B and Supplementary Table 8). Thus, the expression of these genes is lower in the MVP region, indicating that

the MVP region may have an impaired regulation of circulation and alteration in plasma membrane transport. Interestingly, several genes expressed by normal EC (e.g. *ANXA3, SLC1A1, PTPRR, LY6E*) are not enriched in the MVP region (Supplementary Figure 5A, C and Supplementary Table 8). Genes downregulated in GBM EC but highly expressed in MVP region (119 genes) are defining GO gene sets associated with vascular development (Supplementary Figure 5A, D and Supplementary Table 8). This gene cluster contains EC genes which expression is not lost by EC in MVP but whose expression is relatively lower when compared to normal EC, and are encoding for transcription factors, cell-cell contact and cell adhesion molecules, and arterial endothelial cell markers (Supplementary Figure 5E, Supplementary Table 8). Genes upregulated in GBM EC and also highly enriched in LE and IT regions (132 genes) in the IVY GAP dataset were associated with neuronal signaling (e.g. signal release, glutamatergic synaptic transmission, axonogenesis) (Supplementary Figure 5F-H and Supplementary Table 8). These alterations localizing to LE and IT regions could be a sign of an altered neuronal signaling induced by the tumor cells surrounding blood vessels, which in turn promotes glioma progression [21,22]. Genes upregulated (157 genes) in GBM EC and preferentially expressed in MVP region included genes defining GO-gene sets describing extracellular matrix (ECM) (Supplementary Figure 5F, I, J and Supplementary Table 8). This analysis suggests that alterations in GBM blood vessels vary according to anatomical region.

Comparison of DEG in GBM vasculature with published datasets

We next compared DEG in GBM vasculature identified in our dataset with published data where gene expression alterations were identified in GBM vasculature using different approaches [19,20]. Dusart et al. used a bioinformatics-based approach to identify human malignancy-associated EC changes *in silico* using bulk RNA sequencing data from normal human cortex, low-grade glioma and glioblastoma [20]. Out of these 42 malignancy-associated EC genes, 41 genes were expressed in our dataset, and 9 genes were significantly up-regulated in GBM samples compared to control (*NOX4, COL4A1, COL4A2*, *ANGPT2*, *TNFRSF4, ACE, ENPEP, LAMC3, EXOC3L2*) (Supplementary Figure 9A). Five out of these 9 genes (*ENPEP, LAMC3, EXOC3L2, TNFRSF4, NOX4)* belong to the 10 predicted GBM-EC markers identified by Dusart et al. [20]. In addition, Dusart et al. identified 121 genes that were usually expressed in healthy EC but were downregulated in GBM EC. Thirty-seven of these genes were significantly downregulated in our GBM samples, e.g. *SLC2A1*, *ABCB1, LSR, ANXA3, GATA2, SHE, PAQR5, BMP6,*

PGR (Fig. 1A, Supplementary Figure 9B, Supplementary Table 9). Two of these genes, *SLC2A1* and *ABCB1,* have been previously implicated in the BBB function. Interestingly, in the IVY GAP dataset, the downregulated gene *ANXA3* shows a higher expression in LE+IT regions that have a relatively “normal” vasculature, whereas *SHE* and *GATA2* show a higher expression in the MVP region (Supplementary Figure 5C, Supplementary Table 8). Two GBM samples in our dataset (#3 and #9) had a high enrichment score for the GBM-EC signature identified by Dusart et al. (Supplementary Figure 9C). The enrichment score for normal brain-EC enriched transcripts identified by Dusart et al. was highest in control samples (Supplementary Figure 9D).

Dieterich et al. analyzed the transcriptome of vessels isolated by laser microdissection from non-malignant brain, low-grade glioma and GBM using Affymetrix microarrays [19]. Out of 78 genes identified by Dieterich et al. as being upregulated in GBM vessels compared to low-grade glioma and control vessels, 24 genes were significantly upregulated also in our dataset (Supplementary Figure 9E, F). Interestingly, all 24 genes, except for *CA2, WEE1, LOXL2*, and *ANKRD10*, are higher expressed in the IVY GAP dataset in the MVP region (Supplementary Table 8). Expression of five genes (*NOX4, COLA41, COL4A2, ENPEP* and *ANGPT2)* out of the 24 was shown to be upregulated by GBM vasculature also by Dusart et al. [20]. In addition, two genes (*CFH* and *GIMAP8*) identified as upregulated in Dieterich et al. were downregulated in our dataset (Supplementary Figure. 9E). This could be due to the different methods (Affymetrix vs RNA sequencing) to detect gene expression changes. Out of 16 downregulated genes in Dieterich et al, 5 were downregulated in our dataset (*PGR, RAMP2, TRPM6, RERGL, PDCD4*) (Supplementary Figure 9E). *PGR* was also identified as a downregulated gene in GBM EC by Dusart et al [20]. Interestingly, a lack of PGR expression has been shown to increase vascular response to injury [23]. Finally, three samples in our dataset (#3, #9, #27) had a high enrichment score for the GBM signature identified by Dieterich et al., (Supplementary Figure 9F) [19].

Comparison of DEG in GBM and BM vasculature

We next compared DEG in GBM and BM vasculature identified in our study. Out of all DEG in the GBM and BM dataset, 556 genes were deregulated in both tumor types when compared to control samples (Supplementary Figure 11A-D). GO over-representation analysis using genes upregulated in both BM and GBM EC showed deregulation of genes implicated in angiogenesis and ECM deposition (Supplementary Figure 11D, Supplementary Table 10). Genes upregulated only in GBM were enriched

in gene sets related to axon development, trans-synaptic signaling, and cell motility (Supplementary Figure 11E, Supplementary Table 10). No specific gene set was significantly enriched when analysing genes upregulated only in BM or when using genes downregulated in both GBM and BM, indicating that these genes were not grouped within specific functions or pathways. Finally, GO overrepresentation analysis of genes downregulated in either one or the other tumor type revealed downregulation of gene sets related to angiogenesis, endothelial migration and response to interferon-gamma in GBM EC (Supplementary Figure 11F, Supplementary Table 10), and regulation of transmembrane membrane transport in BM EC (Supplementary Figure 11G, Supplementary Table 10).

BBB dysfunction module

We next investigated whether GBM and adenocarcinoma metastasis EC showed deregulation of a generic “BBB dysfunction module” identified by analyzing 4 different mouse brain pathologies resulting in a BBB dysfunction (increased vascular permeability) [18]. Out of 136 genes defining the “BBB dysfunction module” in mouse, 124 and 105 homologous genes were found in human GBM and BM EC, respectively, and 54 and 46 genes were significantly deregulated in the GBM and BM, respectively (Supplementary Figure 11H, I). The BBB dysfunction module genes were significantly enriched in both datasets (Supplementary Figure 11J, K). The majority of upregulated genes are implicated in angiogenesis (*ROBO1, APLNR*), cell migration (*HMMR, DPYSL3*) and cell proliferation (*TOP2A, TPX2, MKI67*), and extracellular matrix deposition and modification (*TNC, ADAM12, COL1A1, COL3A1, LOXL2*). Some “BBB dysfunction module” genes were downregulated, with *CYP1B1* being downregulated in both datasets (Supplementary Figure 11H, I). Several of these genes are expressed in the normal mouse brain mostly by vessel-associated fibroblasts (*CYP1B1, ITITM1, IGSF10, S100A6, SULF1, SERPING1*). The expression of some fibroblast markers is upregulated in GBM vasculature (Fig. 3 and Supplementary Figure 10), which could reflect changes in the profile of vessel-associated fibroblasts in the tumor tissue. Both GBM and BM blood vessels show alterations in genes defining the “BBB dysfunction module”, thus indicating changes in cellular and ECM composition, and cell quiescence.

Supplementary figure legends and tables

Supplementary Figure 1. Preoperative gadolinium-enhanced T1-weighted magnetic resonance images of patients. A. MRI scans of GBM patients. **B**. MRI scans of patients with lung metastases. Yellow arrowheads point to gadolinium enhanced tumor tissue. Patient numbers refer to patients described in Supplementary Table 3.

Supplementary Figure 2. **EC isolation strategy, clustering and cell type enrichment analysis. A.** Workflow to enrich EC from either a control brain or from a brain tumor surgery material using an immunoprecipitation approach. Dissociated samples were first incubated with a mix of anti-CD45 and anti-CD15 antibody conjugated magnetic beads to remove CD31 expressing blood cells [24,25]. This was followed by a positive selection using anti-CD31 antibody conjugated magnetic beads. $CD31^+$ EC enriched samples were subjected to RNA seq. Unsupervised clustering of RNA seq data of individual samples derived from GBM and normal brain vasculature (**B**) and BM and normal vasculature (**C**) using Poisson distance of non-normalized counts. **D.** GSEA using cell-type specific gene sets did not identify a significant enrichment of vascular and brain cell-type specific genes [26] in DEG in BM vasculature compared to normal brain vasculature.

Supplementary Figure 3. GBM and control samples are enriched for endothelial cells. Expression of 25 individual EC core genes [16] in EC isolated from GBM and control brain (Ctrl), and in different bulk brain regions. Ctx - Cortex, Hc - hippocampus, Pt - putamen). The bulk RNA seq data was obtained from the GTEx project.

Supplementary Figure 4. BM and control samples are enriched for endothelial cells. Expression of 25 individual EC core genes [16] in EC isolated from the BM and control brain (Ctrl), and in different bulk brain regions (GTEx project). Ctx - Cortex, Hc - hippocampus, Pt - putamen). The bulk RNA seq data was obtained from the GTEx project.

Supplementary Figure 5. Distribution of expression of DEG in GBM vasculature in different GBM tumor regions. **A.** Relative standing (row z-score) expression of downregulated genes in GBM

EC in different GBM regions (LE, IT, MVP) in the IVY GAP dataset [12]. The green square and the red square surround gene clusters preferentially expressed in LE and IT, and in the MVP region, respectively. **B, D.** GO overrepresentation analysis of downregulated genes in GBM EC enriched in LE and IT (**B**) and in MVP (**D**) regions in the IVY GAP dataset. **C, E.** Examples of genes defining biological processes enriched in LE and IT (**C**) and in MVP (**E**) regions (see B, D and STable 8). **F.** Relative standing (row z-score) expression of upregulated genes in GBM EC in different GBM regions (LE, IT, MVP) in the IVY GAP dataset. The light green square and the pink square surround gene clusters preferentially expressed in LE and IT, and in the MVP region, respectively. **G, I.** GO overrepresentation analysis of upregulated genes in GBM EC enriched in LE and IT (**G**) and in MVP (**I**) regions in the IVY GAP dataset. **H, J.** Examples of genes defining biological processes enriched in LE and IT (**G**) and in MVP (**I**) regions (see G, I and STable 8). LE-leading edge, IT-infiltrating tumor, MVP-microvascular proliferation region.

Supplementary Figure 6. Expression level of upregulated genes in GBM ECs in the IVY GAP dataset. Heatmap of expression (row z-score) of upregulated genes in GBM EC in different anatomical regions in the IVY GAP dataset [12]. CT - cellular tumor, IT - infiltrating tumor, LE - leading edge, CTpan - pseudopalisading cells around necrosis, CTmvp - microvascular proliferation region.

Supplementary Figure 7. Expression level of downregulated genes in GBM ECs in the IVY GAP dataset. Heatmap of expression (row z-score) of downregulated genes in GBM EC in different anatomical regions in the IVY GAP dataset [12]. CT - cellular tumor, IT - infiltrating tumor, LE - leading edge, CTpan - pseudopalisading cells around necrosis, CTmvp - microvascular proliferation region.

Supplementary Figure 8. Deregulated transporters and ECM components in GBM and BM vasculature. Deregulated SLC transporters (**A**, **C**) and ECM components (**B**, **D**) in GBM (**A**, **B**) and BM (**C**, **D**). An asterix marks genes previously reported deregulated in GBM vasculature. **F**- **M**. Expression of DEG in brain tumor vasculature in mouse brain vascular cells according to Vanlandewijck et al. [26]. PC - Pericytes; SMC - Smooth muscle cells; MG - Microglia; FB - Vascular

fibroblast-like cells; OL - Oligodendrocytes; EC - Endothelial cells; AC - Astrocytes; v - venous; capil - capillary; a - arterial; aa - arteriolar; 1,2,3- subtypes.

Supplementary Figure 9. Comparison of DEGs in GBM EC with published datasets. Volcano plots showing DEG in GBM vasculature. Marked are malignancy-associated EC genes, which had a correlation score to a set of known EC markers above 0.5 for GBM and below 0.5 for normal brain (**A**) and normal brain EC-specific genes (**B**) defined by Dusart et al. [20] in GBM EC compared to the control samples. Sum of mean z-scores (enrichment score) of the malignancy-associated endothelial genes (**C**) and normal EC-specific genes (**D**) in individual GBM and control samples. (**E**) Volcano plots showing DEG in GBM vasculature. DEG identified by Dieterich et al. [19] are marked. Colors show deregulation of genes in Dieterich et al.: green square – upregulated, yellow square – downregulated. (**F**) Sum of mean z-scores (enrichment score) of DEG identified by Dietrich et al. in individual control and GBM EC enriched samples.

Supplementary Figure 10. Cell-type specific expression of DEG in GBM vascular fragments. Expression of *Adam12* (**A**), *Depep1* (**B**), *Clec3b* (**C**) and *Fbln2* (**D**) in adult mouse brain vascular cells. RNA expression levels of *DPEP1* (**E**) and *FBLN2* (**F**) in GBM and normal brain EC. Expression of *Col1a1* (**G**), *Tgfbi* (**H**), and *Lamb1* (**I**) in adult mouse brain vascular cells. Expression data presented in **A**-**D** and **G**-**I** are from Vanlandewijck et al. [26]. *In situ* hybridization images showing expression of *COL1A1* (**J**), *TGFBI* (**K**), *LAMB1* (**L**) in human GBM tissue. Black arrowheads point to cells adjacent to vasculature; red arrowheads point to positive cells in the parenchyma. Scale bar – 100 µm. *In situ* hybridization images are from Allen Institute for Brain Science, Ivy Glioblastoma Atlas Project. Sample information: COL4A1 -W12-1-1-E, 100122370; TGFBI - W11-1-1-B, 311176994; LAMB1 - W12-1-1-E, 100122005; PLVAP - W11-1-1-E, 100120667. PC - Pericytes; SMC - Smooth muscle cells; MG - Microglia; FB - Vascular fibroblast-like cells; OL - Oligodendrocytes; EC - Endothelial cells; AC - Astrocytes; v - venous; capil - capillary; a - arterial; aa - arteriolar; 1,2,3- subtypes.

Supplementary Figure 11. Identification of common DEG in GBM and BM EC and identification of deregulated BBB dysfunction module genes. Venn diagrams showing the total number of common DEG (**A**), upregulated genes only (**B**), downregulated genes only (**C**) between the GBM and BM vasculature. GO overrepresentation analysis (biological processes) of genes upregulated both in the GBM and BM vasculature (**D**), upregulated only in GBM (**E**), downregulated only in GBM (**F**), downregulated only in BM (**G**). Volcano plots showing the change of expression of the BBB dysfunction module genes in GBM (**H**) and BM (**I**) vasculature compared to the normal vasculature. **J-K.** Sum of mean z-scores (enrichment score) of the BBB dysfunction module genes in individual GBM (**J**) and BM (**K**) samples and control samples. The BBB dysfunction module genes are from Munji et al. [18].

Supplementary Figure 12. **Alterations in the vasculature of the GBM and BM.** Pie charts showing different BBB features and the extent of deregulation in the GBM (**A**) and BM (**B**) vasculature. Genes labelled in red are upregulated, in blue are downregulated. The color scheme shows the extent of alterations in each BBB feature: green – no alterations, yellowish – few alterations, orange – modest alterations, violet – extensive alterations. (**C**) Biological processes deregulated both in the GBM and BM vasculature. (**D**) Alterations in brain tumor vasculature that could be hijacked to improve drug delivery into tumor. Biopharmaceuticals could enter the brain via receptor-mediated transcytosis (1) or permeable cell-cell junctions (2). However, junctional permeability is heterogeneous (2*). Both GBM and BM vasculature show upregulation of INSR. Exploiting INSR-mediated transcytosis to deliver biopharmaceuticals could potentially be exploited to deliver drugs into brain tumors. ABC transporters (3) limit the availability of lipophilic drugs. Brain tumor vasculature shows upregulation of *ABCC3* (MRP3) associated with chemotherapy resistance. Tumor vasculature shows deregulation of several SLC transporters, which could be exploited for targeted drug delivery (4) (e.g. amino acid transporters, and nucleobase and nucleoside transporters). In addition, altered expression of SLC transporters could indicate an altered metabolic need of GBM endothelial cells (5), or metabolic cooperation between EC and tumor cells. Metabolic alterations could be exploited to target tumor metabolism. Of note, GBM vasculature shows reduced expression of vital glucose transporter – SLC2A1. Modification of ECM surrounding tumor blood vessels (6) could enhance response to chemotherapy. Vessel-associated fibroblast like cells (7) in brain tumors, similar to cancer-associated fibroblasts in peripheral

tumors, could mediate resistance to various anti-cancer therapies, including immunotherapy. Low expression level of leukocyte adhesion molecules on brain tumor vasculature might further impede successful immunotherapy (8).

Supplementary Table 1. Primary antibodies used for immunohistochemistry.

Target	Host	Company	Catalogue #	Dilution
CD31	mouse	Abcam	ab119339	1:100
GFAP	goat	Abcam	ab53554	1:100
SLC36A1	rabbit	Abcam	ab189441	1:200
INSR	rabbit	Abcam	ab5500	1:200
CLEC3B	rabbit	Abcam	ab108999	1:100
ADAM12	rabbit	ThermoFisher	PA583163	1:100

Supplementary Table 3. Clinical features of patients enrolled into study.

Sample_ ID	Sex	Age	Sample type	Diagnosis	MGMT	Location	Therapy prior surgery
RNA sequencing							
3	M	70	GBM	IDH1 wt	met	Right frontal	None
8	M	55	GBM	IDH1 wt	n met	Right parietal	None
9	M	66	GBM	IDH1 wt	n met	Left fronto-temporal	Dexamethasone
27	F	66	GBM	IDH1 wt	n met	Right tempo-parietal	Dexamethasone
29	M	69	GBM	IDH1 wt	met	Left occipital	None
6	M	5	Control	Epilepsy	-	Left temporal, amygdala, hippocampus	-
11	F	82	Control	Autopsy	-	Left temporal	-
12	F	73	Control	Autopsy	-	Left temporal	-
14	M	64	Control	Autopsy	-	Left temporal	-
15	M	66	Control	Autopsy	-	Left temporal	-
26	M	16	Control	Epilepsy	-	Left temporal (2/3 resection)	-
16	F	32	BM	adenocarcinoma metastasis	-	Right temporo-parietal	Dexamethasone, Chemotherapy** (Cetuximab, FOLFOX, FOLFIRI)
22	M	70	BM	adenocarcinoma metastasis	-	Left cerebellar	Dexamethasone, Chemotherapy** (Carboplatin, Pemetrexed)
23	F	66	BM	adenocarcinoma metastasis	-	Left parietal	Chemotherapy** (Cisplatin, Docetaxel)
28	M	59	BM	adenocarcinoma metastasis	-	Right frontal	Dexamethasone, Chemotherapy** (Axitinib, Sunitinib)

30	F	47	BM	adenocarcinoma metastasis	-	Left frontal	Dexamethasone
Immunohistochemistry							
59	M	74	GBM	IDH1 wt	n met	Left frontal	Dexamethasone
60	F	69	GBM	IDH1 wt	n met	Right frontal	Dexamethasone
68	M	70	GBM	IDH1 wt	n met	Right temporal	Dexamethasone
69	F	51	GBM	IDH1 wt*	NA	Left frontal	Chemoradiotherapy (Temozolomid)
14	M	64	Control	Autopsy	-	Left temporal	-
53	F	64	Control	Autopsy	-	Left temporal	-
54	M	67	Control	Autopsy	-	Left temporal	-
56	M	72	Control	Autopsy	-	Left temporal	-

GBM - glioblastoma multiforme, IDH1 - isocitrate dehydrogenase 1, BM - brain metastasis, MGMT - O[6]-methylguanine-DNA methyltransferase, met - methylated, n met - not methylated, NA - not analyzed.

* Diagnosis by histochemistry: wt, diagnosis by sequencing: R132H mutant

**treatment of primary tumor

Supplementary Table 2. Quality control of RNA sequencing data.

Supplementary Table 4. DEG in GBM vasculature compared to normal brain vasculature.

Supplementary Table 5. DEG in BM vasculature compared to normal brain vasculature.

Supplementary Table 6. Overrepresented GO biological process gene sets in upregulated and downregulated genes of GBM vasculature.

Supplementary Table 7. Overrepresented GO biological process gene sets in upregulated and downregulated genes of BM vasculature.

Supplementary Table 8. Overrepresented GO biological process gene sets in DEG in GBM vasculature preferentially expressed in different tumor regions region in IVY GAP [12]. Up- and downregulated genes and niche defining genes listed according to preferential expression in tumor regions. LE - leading edge, IT - infiltrating tumor, MVP - microvascular proliferation region.

Supplementary Table 9. Expression of genes identified by Dusart et al.[20] and Dietrich et al.[19] in our GBM dataset.

Supplementary Table 10. Overrepresented GO biological process gene sets of genes that are up- or downregulated both or only in GBM and BM vasculature compared to normal vasculature.

References

1. Bolger AM, Lohse M, Usadel B. Trimmomatic: a flexible trimmer for Illumina sequence data. *Bioinformatics (Oxford, England).* 2014; 30(15):2114-2120.

2. Dobin A, Davis CA, Schlesinger F, et al. STAR: ultrafast universal RNA-seq aligner. *Bioinformatics (Oxford, England).* 2013; 29(1):15-21.

3. Li H, Handsaker B, Wysoker A, et al. The Sequence Alignment/Map format and SAMtools. *Bioinformatics (Oxford, England).* 2009; 25(16):2078-2079.

4. Liao Y, Smyth GK, Shi W. The R package Rsubread is easier, faster, cheaper and better for alignment and quantification of RNA sequencing reads. *Nucleic acids research.* 2019; 47(8):e47.

5. Love MI, Huber W, Anders S. Moderated estimation of fold change and dispersion for RNA-seq data with DESeq2. *Genome biology.* 2014; 15(12):550.

6. Ashburner M, Ball CA, Blake JA, et al. Gene ontology: tool for the unification of biology. The Gene Ontology Consortium. *Nature genetics.* 2000; 25(1):25-29.

7. The Gene Ontology Resource: 20 years and still GOing strong. *Nucleic acids research.* 2019; 47(D1):D330-d338.

8. Yu G, Wang LG, Han Y, He QY. clusterProfiler: an R package for comparing biological themes among gene clusters. *Omics : a journal of integrative biology.* 2012; 16(5):284-287.

9. Subramanian A, Tamayo P, Mootha VK, et al. Gene set enrichment analysis: a knowledge-based approach for interpreting genome-wide expression profiles. *Proceedings of the National Academy of Sciences of the United States of America.* 2005; 102(43):15545-15550.

10. Benjamini Y, Hochberg Y. Controlling the False Discovery Rate: A Practical and Powerful Approach to Multiple Testing. *Journal of the Royal Statistical Society. Series B (Methodological).* 1995; 57(1):289-300.

11. Corada M, Orsenigo F, Bhat GP, et al. Fine-Tuning of Sox17 and Canonical Wnt Coordinates the Permeability Properties of the Blood-Brain Barrier. *Circulation research.* 2019; 124(4):511-525.

12. Puchalski RB, Shah N, Miller J, et al. An anatomic transcriptional atlas of human glioblastoma. *Science (New York, N.Y.).* 2018; 360(6389):660-663.

13. Gu Z, Eils R, Schlesner M. Complex heatmaps reveal patterns and correlations in multidimensional genomic data. *Bioinformatics (Oxford, England).* 2016; 32(18):2847-2849.

14. Robinson MD, Oshlack A. A scaling normalization method for differential expression analysis of RNA-seq data. *Genome biology.* 2010; 11(3):R25.

15. Ritchie ME, Phipson B, Wu D, et al. limma powers differential expression analyses for RNA-sequencing and microarray studies. *Nucleic acids research.* 2015; 43(7):e47.

16. Butler LM, Hallstrom BM, Fagerberg L, et al. Analysis of Body-wide Unfractionated Tissue Data to Identify a Core Human Endothelial Transcriptome. *Cell systems.* 2016; 3(3):287-301.e283.

17. Ragusa S, Prat-Luri B, González-Loyola A, et al. Antiangiogenic immunotherapy suppresses desmoplastic and chemoresistant intestinal tumors in mice. *The Journal of clinical investigation.* 2020; 130(3):1199-1216.

18. Munji RN, Soung AL, Weiner GA, et al. Profiling the mouse brain endothelial transcriptome in health and disease models reveals a core blood-brain barrier dysfunction module. *Nature neuroscience.* 2019; 22(11):1892-1902.

19. Dieterich LC, Mellberg S, Langenkamp E, et al. Transcriptional profiling of human glioblastoma vessels indicates a key role of VEGF-A and TGFbeta2 in vascular abnormalization. *J Pathol.* 2012; 228(3):378-390.

20. Dusart P, Hallstrom BM, Renne T, Odeberg J, Uhlen M, Butler LM. A Systems-Based Map of Human Brain Cell-Type Enriched Genes and Malignancy-Associated Endothelial Changes. *Cell reports.* 2019; 29(6):1690-1706.e1694.

21. Venkatesh HS, Morishita W, Geraghty AC, et al. Electrical and synaptic integration of glioma into neural circuits. *Nature.* 2019; 573(7775):539-545.

22. Venkataramani V, Tanev DI, Strahle C, et al. Glutamatergic synaptic input to glioma cells drives brain tumour progression. *Nature.* 2019; 573(7775):532-538.

23. Karas RH, van Eickels M, Lydon JP, et al. A complex role for the progesterone receptor in the response to vascular injury. *The Journal of clinical investigation.* 2001; 108(4):611-618.

24. Bogen SA, Baldwin HS, Watkins SC, Albelda SM, Abbas AK. Association of murine CD31 with transmigrating lymphocytes following antigenic stimulation. *The American journal of pathology.* 1992; 141(4):843-854.

25. Torimoto Y, Rothstein DM, Dang NH, Schlossman SF, Morimoto C. CD31, a novel cell surface marker for CD4 cells of suppressor lineage, unaltered by state of activation. *The Journal of Immunology.* 1992; 148(2):388.

26. Vanlandewijck M, He L, Mae MA, et al. A molecular atlas of cell types and zonation in the brain vasculature. *Nature.* 2018; 554(7693):475-480.

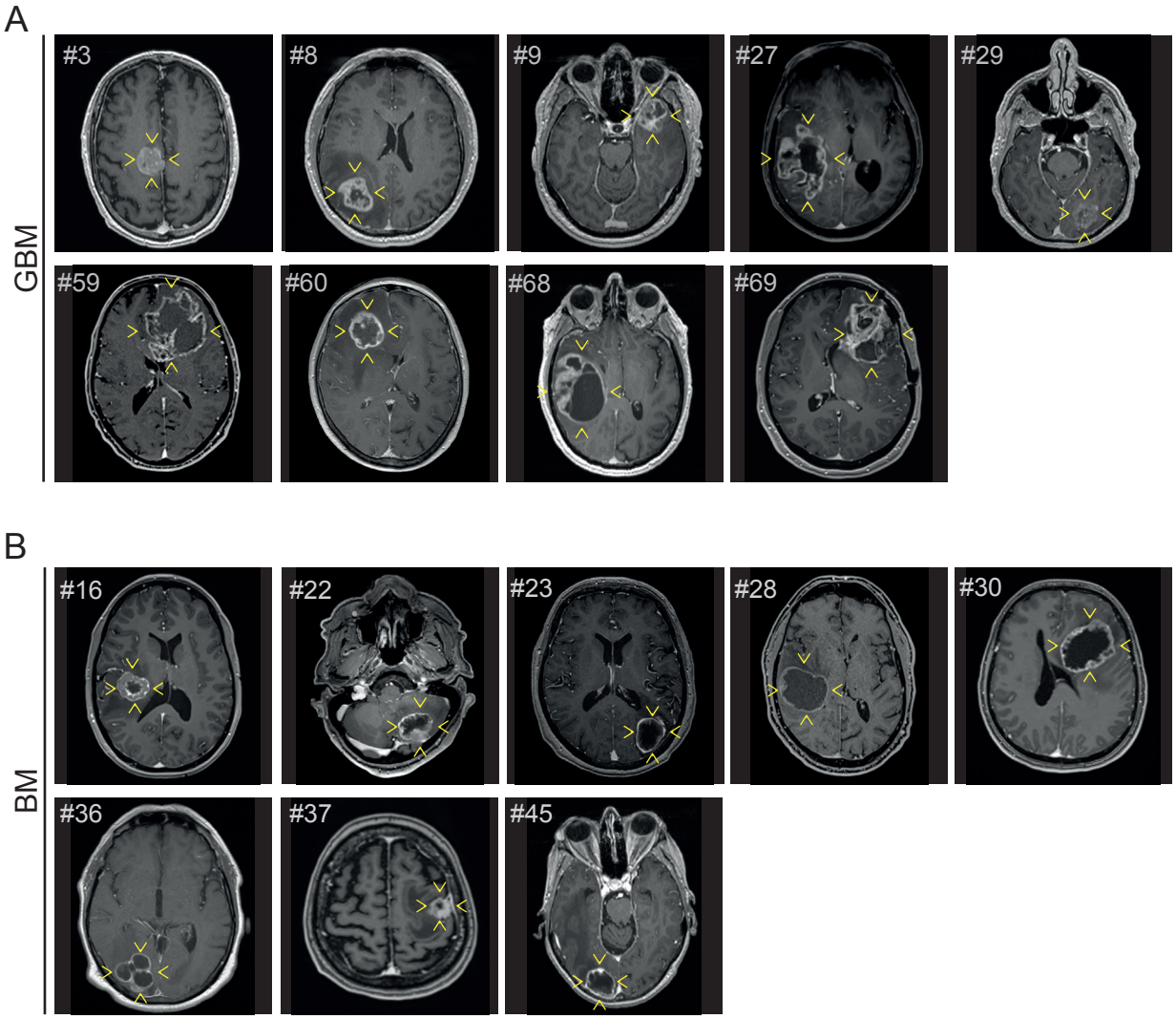
A
GBM
#3
#8
#9
#27
#29
#59
#60
#68
#69
B
BM
#16
#22
#23
#28
#30
#36
#37
#45

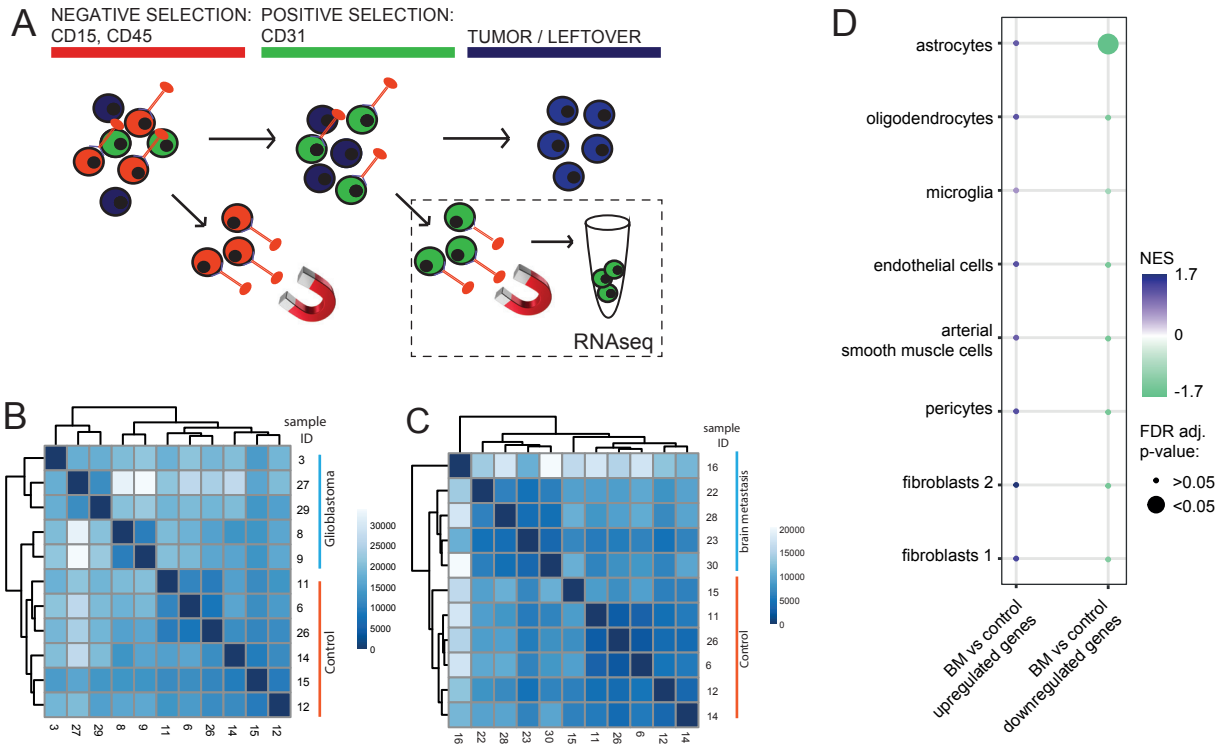
A
NEGATIVE SELECTION:
CD15, CD45
POSITIVE SELECTION:
CD31
TUMOR / LEFTOVER
RNAseq
B
sample ID
Glioblastoma
Control
C
sample ID
brain metastasis
Control
D
astrocytes
oligodendrocytes
microglia
endothelial cells
arterial smooth muscle cells
pericytes
fibroblasts 2
fibroblasts 1
BM vs control upregulated genes
BM vs control downregulated genes
NES
1.7
0
-1.7
FDR adj. p-value:
>0.05
<0.05

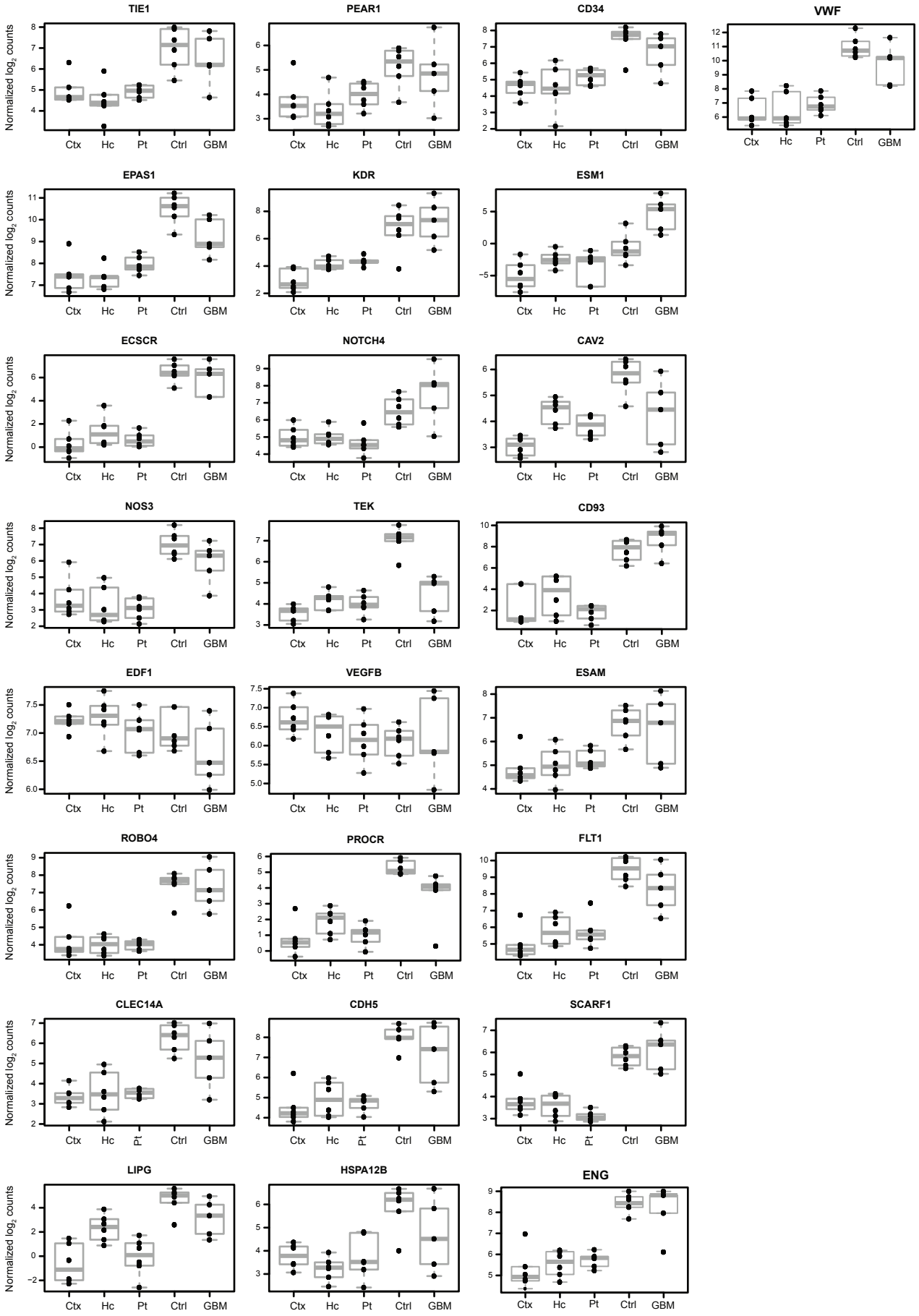
TIE1
PEAR1
CD34
VWF
EPAS1
KDR
ESM1
ECSCR
NOTCH4
CAV2
NOS3
TEK
CD93
EDF1
VEGFB
ESAM
ROBO4
PROCR
FLT1
CLEC14A
CDH5
SCARF1
LIPG
HSPA12B
ENG
Normalized log2 counts
Ctx
Hc
Pt
Ctrl
GBM

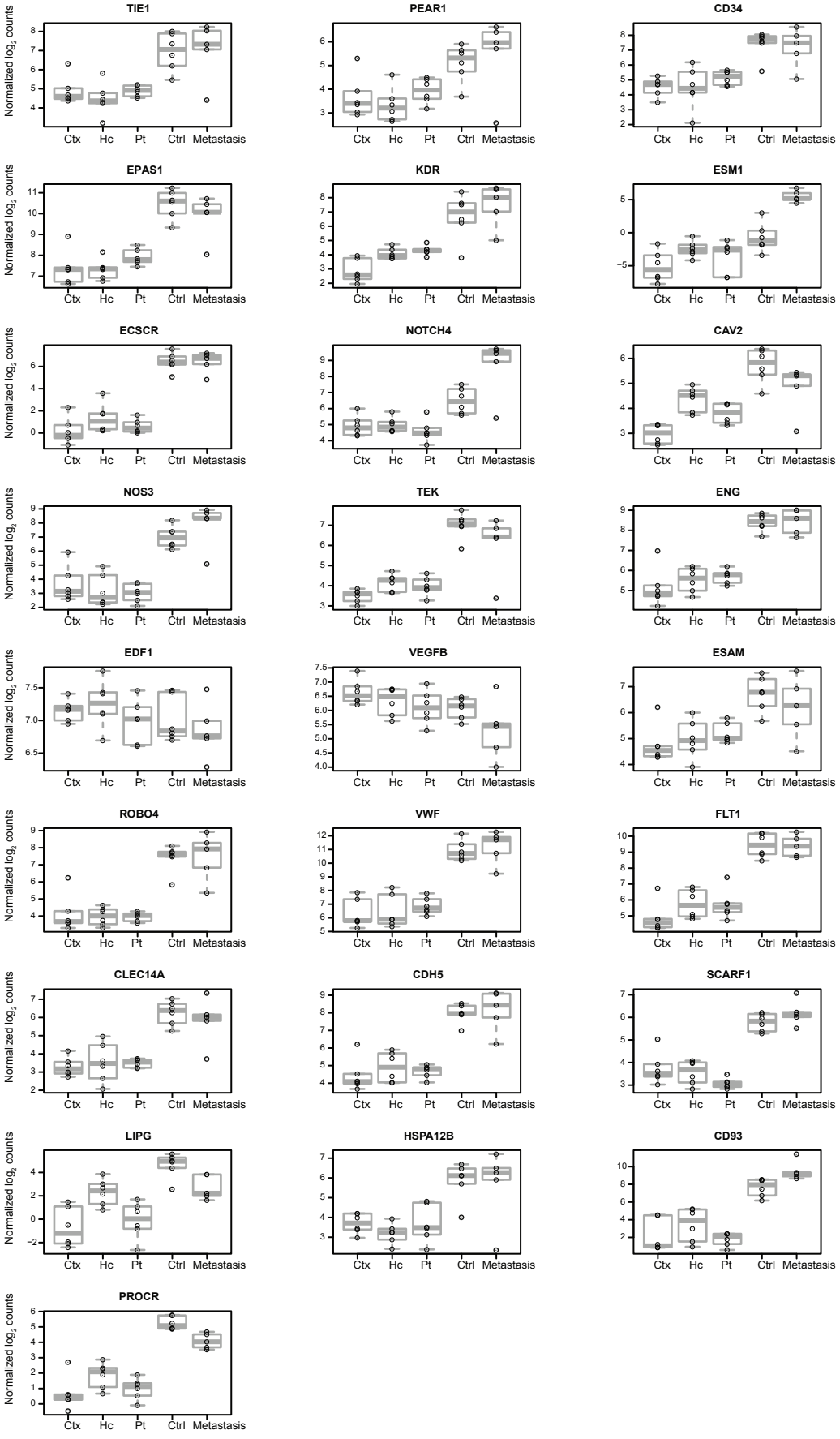
TIE1
PEAR1
CD34
EPAS1
KDR
ESM1
ECSCR
NOTCH4
CAV2
NOS3
TEK
ENG
EDF1
VEGFB
ESAM
ROBO4
VWF
FLT1
CLEC14A
CDH5
SCARF1
LIPG
HSPA12B
CD93
PROCR
Normalized log2 counts
Ctx
Hc
Pt
Ctrl
Metastasis

A GBM vs. Control - downregulated genes

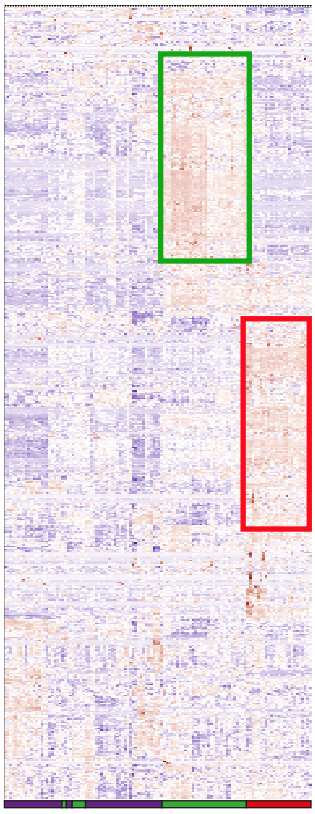

B

downregulated genes - high in LE & IT

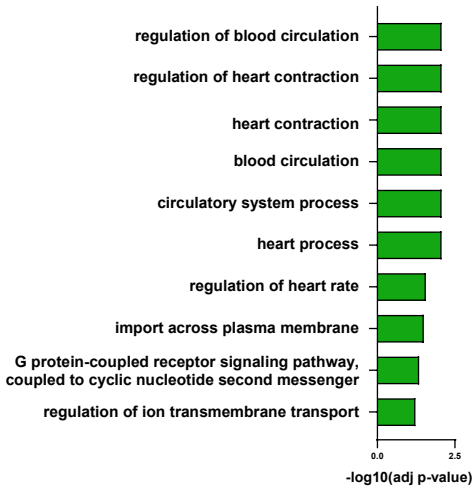

D

downregulated genes - high in MVP

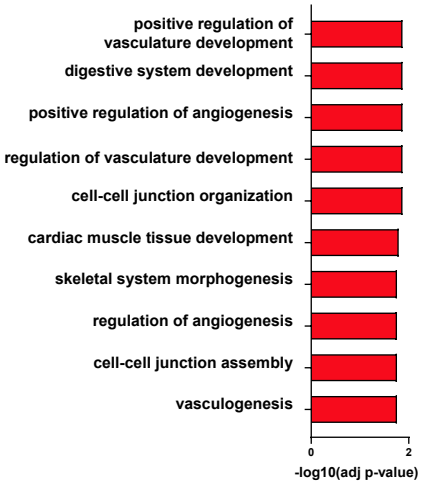

C

ANXA3 ASS1 NOS1 SLC1A1 SLCO1A2 PTPRR

LAMA3 LY6E SLC9A2 ADRB2 BRF2 DDN

SYNE1 GJB6 SLC2A12 TMEM246 IGIP CLIC5

E

ALPL BMX PTPRB GATA2 MARVELD2 GJA5

ZIC3 OCLN HIG1 TGFBR2 TNFSF10 FAT4

RAMP3 SEMA3G RAMP2 SHE RGL4 GIMAP6

F GBM vs. Control - upregulated genes

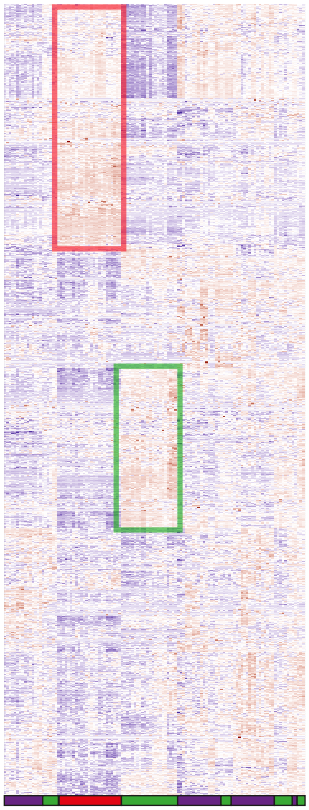

G

upregregulated genes high in LE & IT

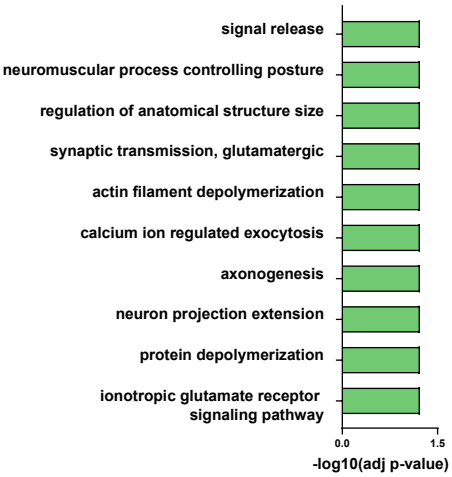

I

upregulated genes - high in MVP

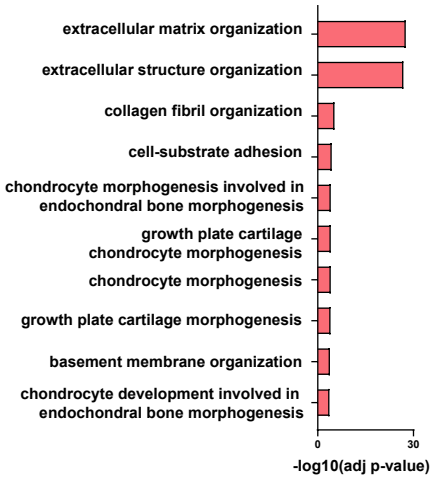

H

PTPRN2 ADD2 SLC1A4 ELK1 NEUROD1 NDP

TNIK SCG5 SYT1 TMEM155 MIB2 KHDC1

USP35 MMEL1 TEX29 CADPS SPRN SOGA3

J

ANGPT2 BMP1 NOX4 COL3A1 COL4A1

COL4A2 ACE PXDN INSR LAMB1 NID1

SPARC PLVAP ESM1 ENPEP SLC36A1

cellular tumor

leading edge & infiltrating tumor (LE & IT)

microvascular proliferation (MVP)

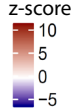


Up−regulated genes
Row z−score
10
5
0
−5

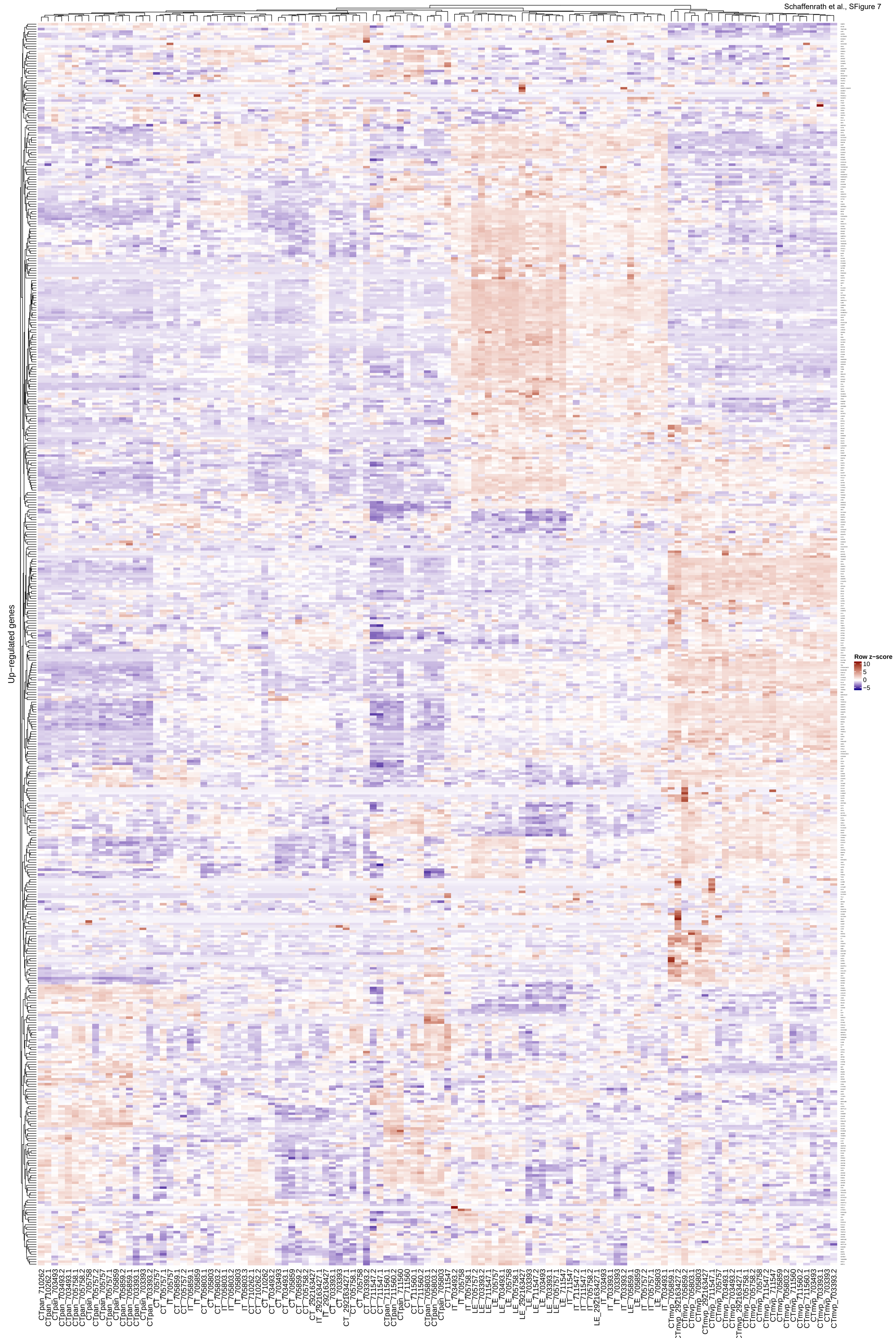
Up−regulated genes
Row z−score
10
5
0
−5
CTpan_710262
CTpan_710262.1
CTpan_703493
CTpan_703493.2
CTpan_703493.1
CTpan_705758.1
CTpan_705758.2
CTpan_705758
CTpan_705757.2
CTpan_705757
CTpan_705757.1
CTpan_705859
CTpan_705859.2
CTpan_705859.1
CTpan_703393.1
CTpan_703393
CTpan_703393.2
CT_705757
CT_705757.1
IT_705757
CT_705859.1
CT_705757.2
IT_705859.1
IT_705859
CT_705803.1
CT_705803
CT_705803.2
IT_705803.1
IT_705803.2
IT_705803
IT_705803.3
CT_710262.1
CT_710262.2
CT_710262
CT_703493.2
CT_703493
CT_703493.1
CT_705859
CT_705859.2
CT_705758.2
CT_292163427
IT_292163427.1
IT_292163427
CT_703393.1
CT_703393
CT_292163427.1
CT_705758.1
CT_705758
CT_703393.2
CT_711547.2
CT_711547.1
CTpan_711560.1
CTpan_711560.2
CTpan_711560
CT_711560.1
CT_711560.2
CTpan_705803.1
CTpan_705803.2
CTpan_705803
CT_711547
IT_703493.2
IT_705758
IT_705758.1
LE_705757.2
LE_703393.2
LE_711547.1
LE_705757
LE_703493.1
LE_705758
LE_705758.1
LE_292163427
LE_703393
LE_711547.2
LE_703493
LE_703393.1
LE_705757.1
LE_711547
IT_711547.2
IT_711547.1
IT_705758.2
LE_292163427.1
IT_703493
IT_703393.1
IT_703393
IT_703393.2
LE_705859.1
LE_705859
IT_705757.2
IT_705757.1
LE_705803
IT_703493.1
CTmvp_705859.1
CTmvp_292163427.2
CTmvp_705859.2
CTmvp_705803.1
CTmvp_705803
CTmvp_292163427
CTmvp_711547.1
CTmvp_705757
CTmvp_703493.1
CTmvp_703493.2
CTmvp_292163427.1
CTmvp_705758.1
CTmvp_705758.2
CTmvp_705758
CTmvp_711547.2
CTmvp_711547
CTmvp_705859
CTmvp_705803.2
CTmvp_711560
CTmvp_711560.2
CTmvp_711560.1
CTmvp_703493
CTmvp_703393.1
CTmvp_703393
CTmvp_703393.2

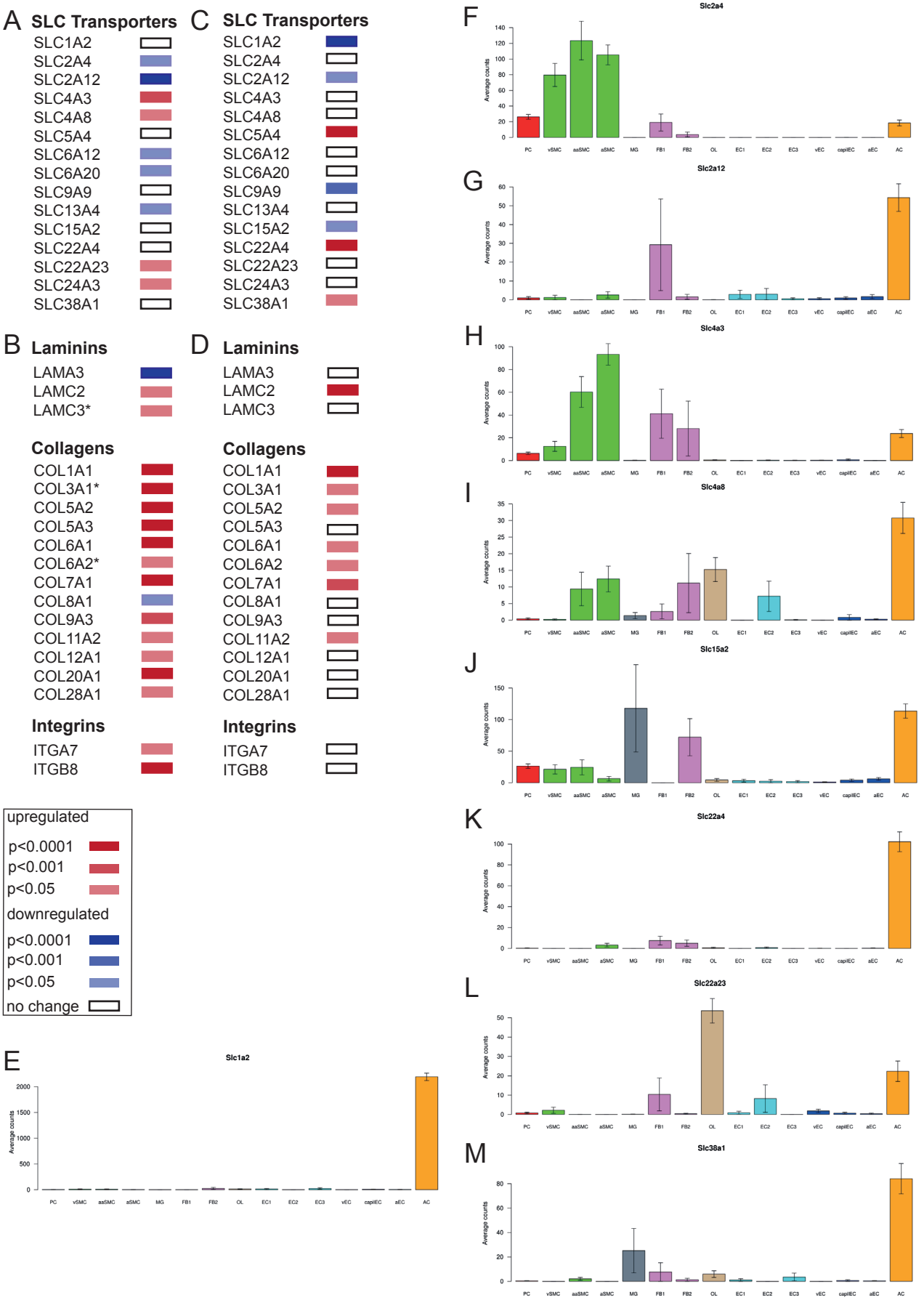
A
SLC Transporters
SLC1A2
SLC2A4
SLC2A12
SLC4A3
SLC4A8
SLC5A4
SLC6A12
SLC6A20
SLC9A9
SLC13A4
SLC15A2
SLC22A4
SLC22A23
SLC24A3
SLC38A1
B
Laminins
LAMA3
LAMC2
LAMC3*
Collagens
COL1A1
COL3A1*
COL5A2
COL5A3
COL6A1
COL6A2*
COL7A1
COL8A1
COL9A3
COL11A2
COL12A1
COL20A1
COL28A1
Integrins
ITGA7
ITGB8
C
SLC Transporters
SLC1A2
SLC2A4
SLC2A12
SLC4A3
SLC4A8
SLC5A4
SLC6A12
SLC6A20
SLC9A9
SLC13A4
SLC15A2
SLC22A4
SLC22A23
SLC24A3
SLC38A1
D
Laminins
LAMA3
LAMC2
LAMC3
Collagens
COL1A1
COL3A1
COL5A2
COL5A3
COL6A1
COL6A2
COL7A1
COL8A1
COL9A3
COL11A2
COL12A1
COL20A1
COL28A1
Integrins
ITGA7
ITGB8
upregulated
p<0.0001
p<0.001
p<0.05
downregulated
p<0.0001
p<0.001
p<0.05
no change
E
Slc1a2
F
Slc2a4
G
Slc2a12
H
Slc4a3
I
Slc4a8
J
Slc15a2
K
Slc22a4
L
Slc22a23
M
Slc38a1
Average counts
PC
vSMC
aaSMC
aSMC
MG
FB1
FB2
OL
EC1
EC2
EC3
vEC
capilEC
aEC
AC

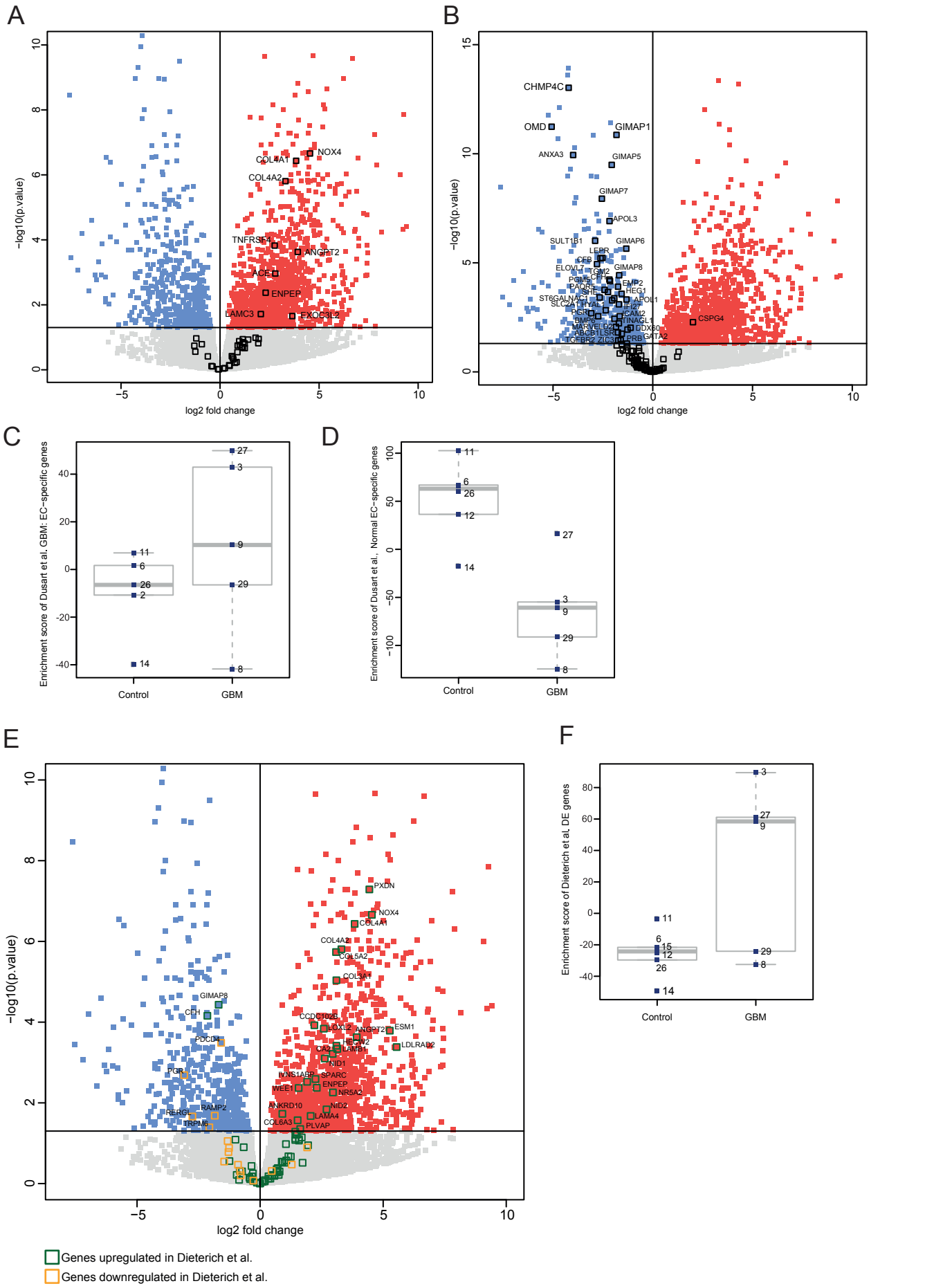
A
B
C
D
E
F
−log10(p.value)
log2 fold change
NOX4
COL4A1
COL4A2
TNFRSF1A
ANGPT2
ACE
ENPEP
LAMC3
EXOC3L2
CHMP4C
OMD
GIMAP1
ANXA3
GIMAP5
GIMAP7
APOL3
SULT1B1
GIMAP6
CSPG4
Enrichment score of Dusart et al. GBM: EC−specific genes
Control
GBM
Enrichment score of Dusart et al.. Normal EC−specific genes
Enrichment score of Dieterich et al. DE genes
PXDN
COL5A2
COL5A1
GIMAP8
CCL14
PDCD4
PGR
RERGL
RAMP2
TRPM6
CCDC102B
LOX12
ANGPT2
ESM1
HEY2
LAMB1
LDLRAD2
NID1
WNS1ABP
SPARC
ENPEP
WEE1
NR5A2
ANKRD10
NID2
COL6A3
LAMA4
PLVAP
Genes upregulated in Dieterich et al.
Genes downregulated in Dieterich et al.

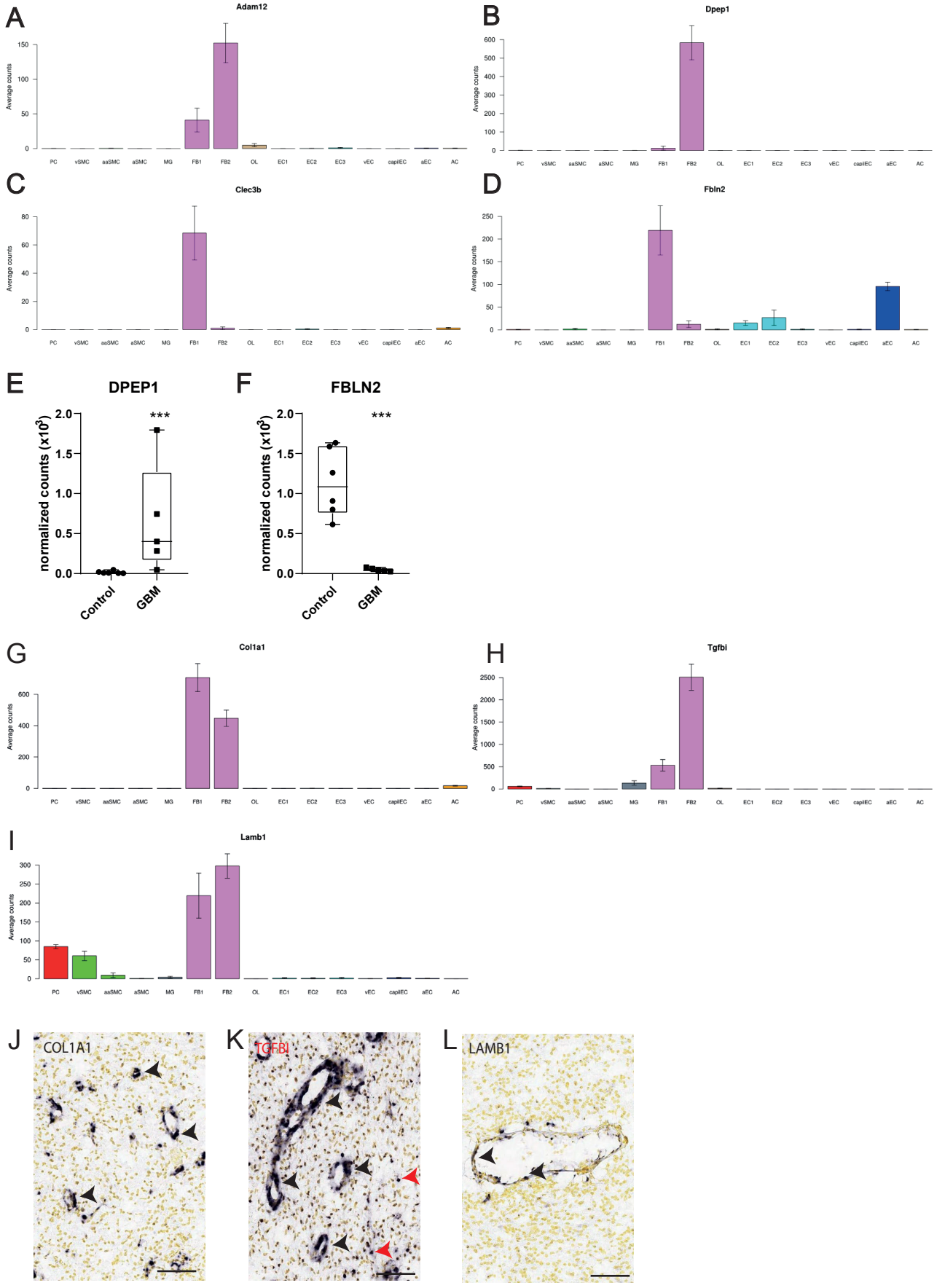
A
Adam12
B
Dpep1
C
Clec3b
D
Fbln2
Average counts
PC vSMC aaSMC aSMC MG FB1 FB2 OL EC1 EC2 EC3 vEC capIEC aEC AC
E
DPEP1
F
FBLN2
normalized counts (x10³)
***
Control
GBM
G
Col1a1
H
Tgfbi
I
Lamb1
J
COL1A1
K
TGFBI
L
LAMB1

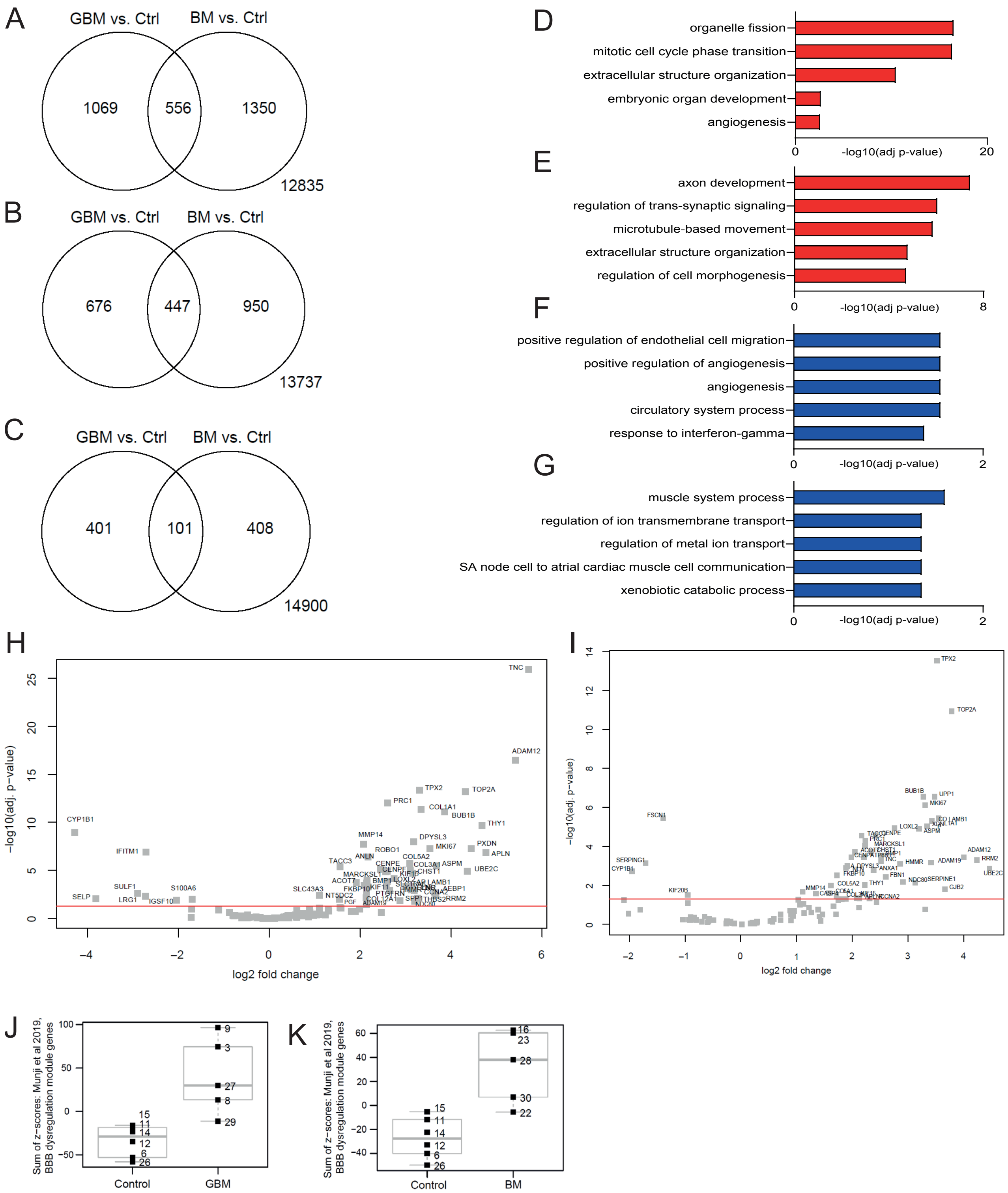
A
GBM vs. Ctrl
BM vs. Ctrl
1069
556
1350
12835
B
GBM vs. Ctrl
BM vs. Ctrl
676
447
950
13737
C
GBM vs. Ctrl
BM vs. Ctrl
401
101
408
14900
D
organelle fission
mitotic cell cycle phase transition
extracellular structure organization
embryonic organ development
angiogenesis
0
-log10(adj p-value)
20
E
axon development
regulation of trans-synaptic signaling
microtubule-based movement
extracellular structure organization
regulation of cell morphogenesis
0
-log10(adj p-value)
8
F
positive regulation of endothelial cell migration
positive regulation of angiogenesis
angiogenesis
circulatory system process
response to interferon-gamma
0
-log10(adj p-value)
2
G
muscle system process
regulation of ion transmembrane transport
regulation of metal ion transport
SA node cell to atrial cardiac muscle cell communication
xenobiotic catabolic process
0
-log10(adj p-value)
2
H
−log10(adj. p−value)
log2 fold change
I
−log10(adj. p−value)
log2 fold change
J
Sum of z−scores: Munji et al 2019, BBB dysregulation module genes
Control
GBM
K
Sum of z−scores: Munji et al 2019, BBB dysregulation module genes
Control
BM

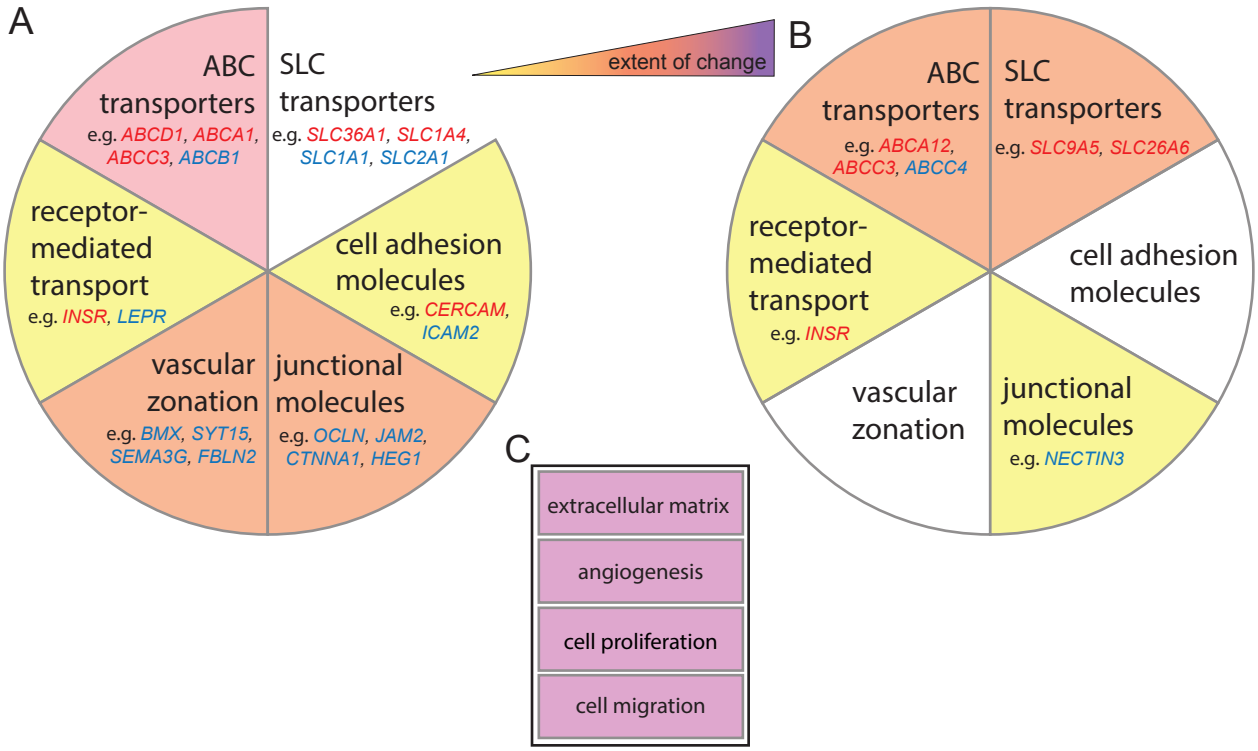
A
ABC transporters
e.g. ABCD1, ABCA1, ABCC3, ABCB1
SLC transporters
e.g. SLC36A1, SLC1A4, SLC1A1, SLC2A1
receptor-mediated transport
e.g. INSR, LEPR
cell adhesion molecules
e.g. CERCAM, ICAM2
vascular zonation
e.g. BMX, SYT15, SEMA3G, FBLN2
junctional molecules
e.g. OCLN, JAM2, CTNNA1, HEG1
extent of change
B
ABC transporters
e.g. ABCA12, ABCC3, ABCC4
SLC transporters
e.g. SLC9A5, SLC26A6
receptor-mediated transport
e.g. INSR
cell adhesion molecules
vascular zonation
junctional molecules
e.g. NECTIN3
C
extracellular matrix
angiogenesis
cell proliferation
cell migration

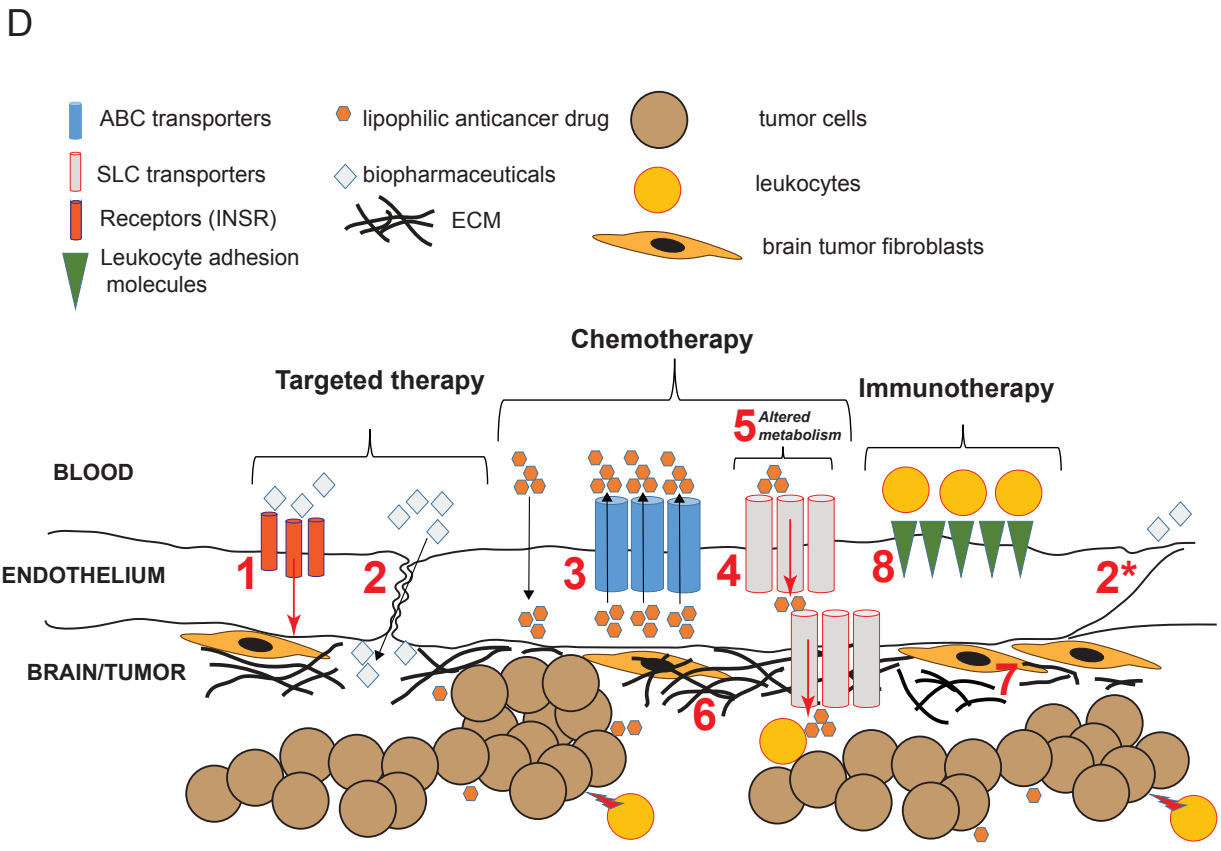
D
ABC transporters
SLC transporters
Receptors (INSR)
Leukocyte adhesion molecules
lipophilic anticancer drug
biopharmaceuticals
ECM
tumor cells
leukocytes
brain tumor fibroblasts
Chemotherapy
Targeted therapy
Immunotherapy
5 Altered metabolism
BLOOD
ENDOTHELIUM
BRAIN/TUMOR
1
2
3
4
8
2*
6
7